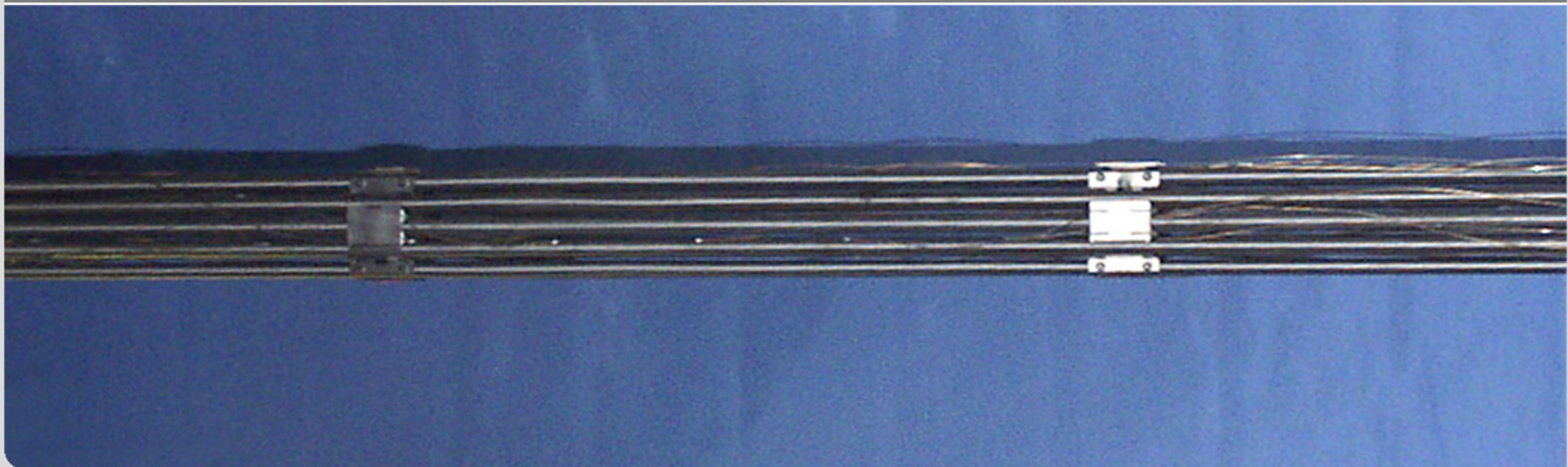


Microstructure and mechanical properties of Zircaloy-4 claddings hydrogenated at temperatures between 900 and 1200 K

A. Pshenichnikov, [J. Stuckert](#), M. Walter

NuMat2014, Florida 2014

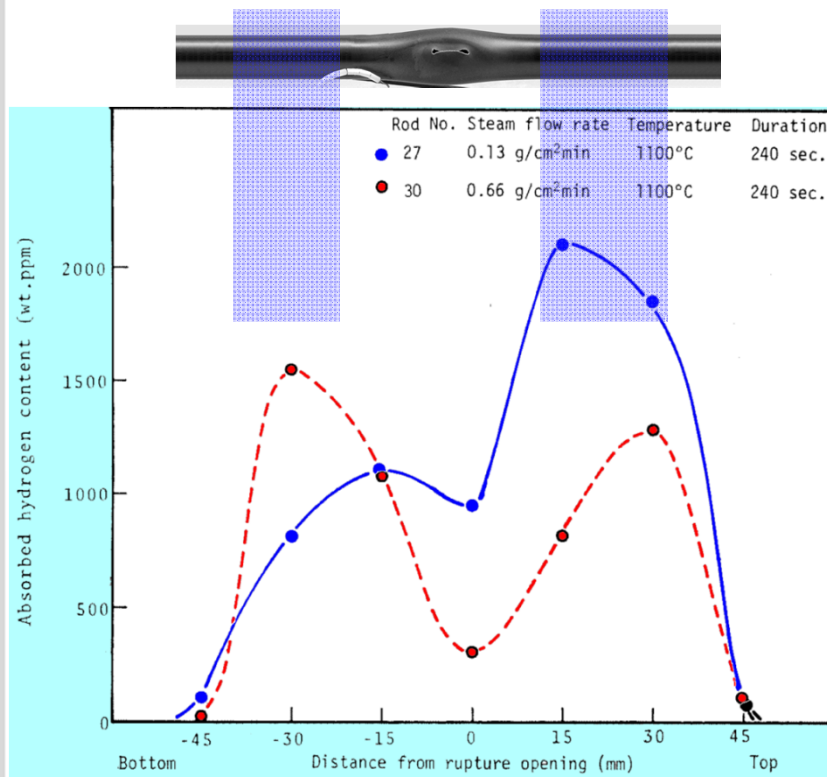
Institute for Applied Materials, IAM-WPT, Program NUKLEAR



Secondary hydriding:

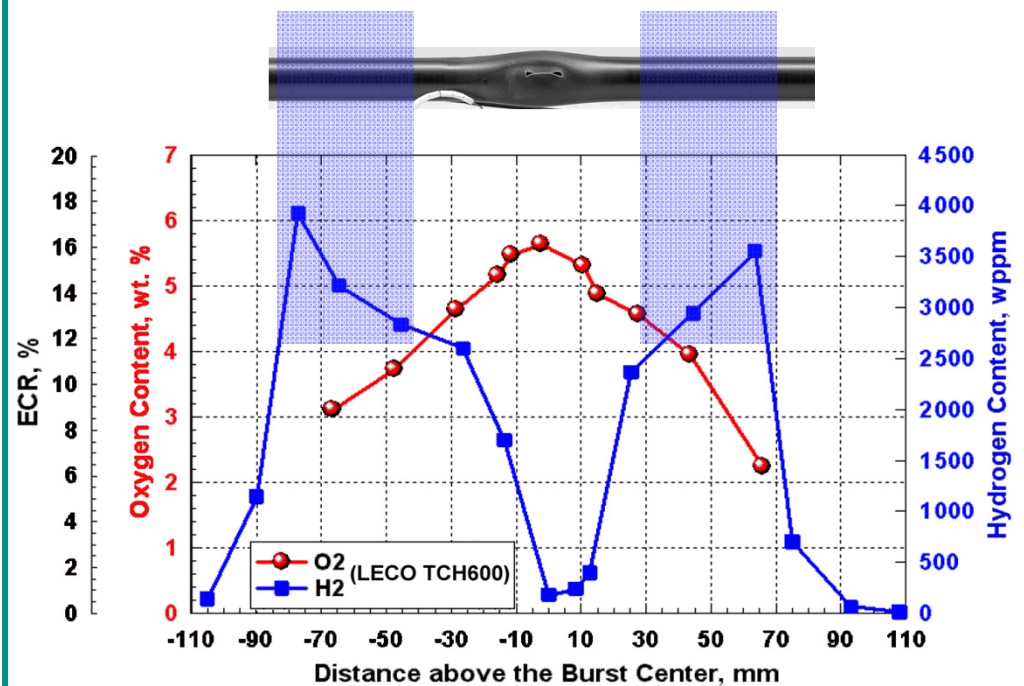
Hydrogen peaks above and below of burst opening

1981, JAERI*: first observation of cladding hydriding by steam ingress through the burst opening



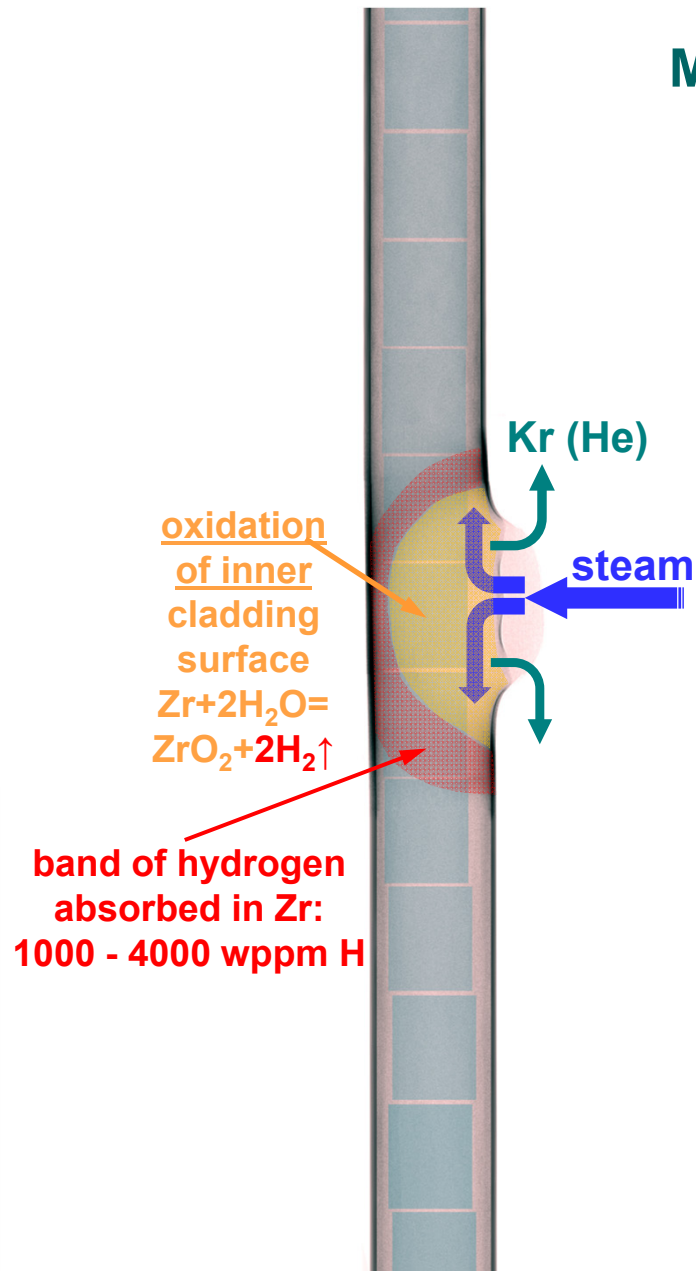
Uetsuka et al., Journal of NUCLEAR SCIENCE and TECHNOLOGY, 18[9], pp. 705~717 (September 1981).

2008, ANL: strong hydriding up to 4000 wppm (significantly higher than ductility limit of 500 wppm)



NUREG-6967 (Billone et al.): unirradiated pressurised sample OCL11 (Zry-2) ramped in steam from 300°C to 1204°C at 5 K/s, held at 1204°C for 300 s, cooled at 3 K/s to 800°C, and cooled from 800°C to RT

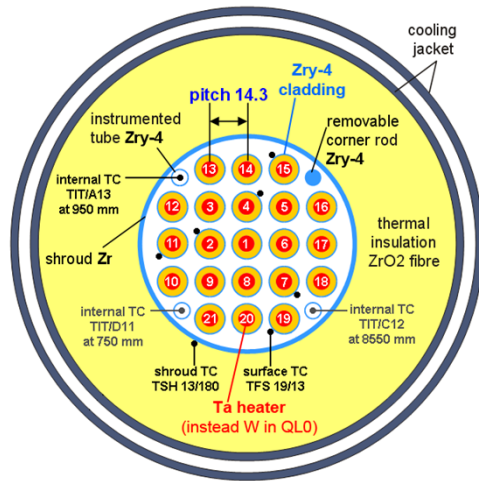
Mechanism of secondary hydriding



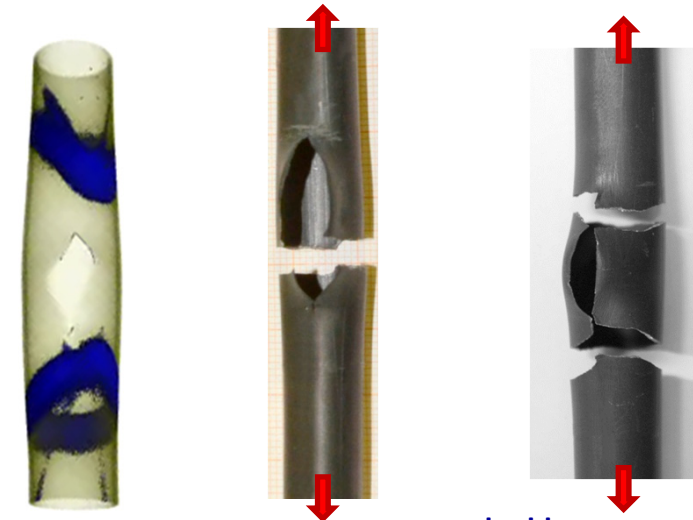
Sequence of phenomena:

- cladding ballooning and burst, relief of inner rod pressure
- steam penetration through the burst opening, steam propagation in decreasing gap between cladding and pellet
- oxidation of inner cladding surface with hydrogen release
- absorption of hydrogen by cladding at the boundary of inner oxidised area at temperatures higher of the phase transition $\alpha \rightarrow (\alpha + \beta)$ in Zr alloy
- local embrittlement of cladding near to burst opening

Bundle experiments of the new QUENCH-LOCA series at KIT



Post-Test Zircaloy-4 clads



hydrogen bands inside cladding detected with n^0 -radiography

rupture of cladding during tensile tests due to stress concentration (rods with $C_H < 1500 \text{ wppm}$)

double ruptures due to hydrogen embrittlement ($C_H > 1500 \text{ wppm}$)

Objective and results

- Investigation of ballooning, burst and secondary hydrogen uptake of the cladding under representative design basis accident conditions
- Detailed post-test investigation of the mechanical properties of the claddings to check the embrittlement criteria and measurement of residual ductility
- Two experiments with Zircaloy-4 bundles (21 electrical heated rods) were performed up to now as commissioning and reference tests
- Four bundle tests with non- and pre-hydrogenated M5[®] and ZIRLO[™] claddings will be performed up to 2015

Experimental procedure for single clad tests



Hydrogenation facility
LORA furnace

Hydrogen gas partial
pressure: 0.1 bar



Specimen before
hydrogenation



Specimen withdrawal in air
after hydrogenation

Estimated cooling rate:
5 K/s



Cooled specimen
after hydrogenation

H₂ duration:
2 to 12 minutes

Material and methods of accompanying single effect test

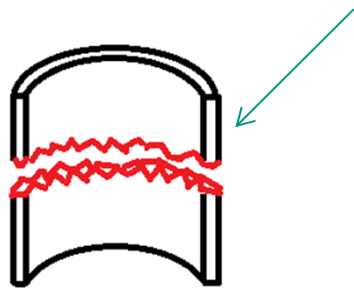
Material: Conventional Zircaloy-4 cladding tube

ICP-OES measurement of Zircaloy-4 chemical composition (by weight):

Sn: $1.33 \pm 0.02\%$, Fe: $0.23 \pm 0.002\%$, Cr: $0.12 \pm 0.0003\%$, O: $0.116 \pm 0.003\%$, Zr balance

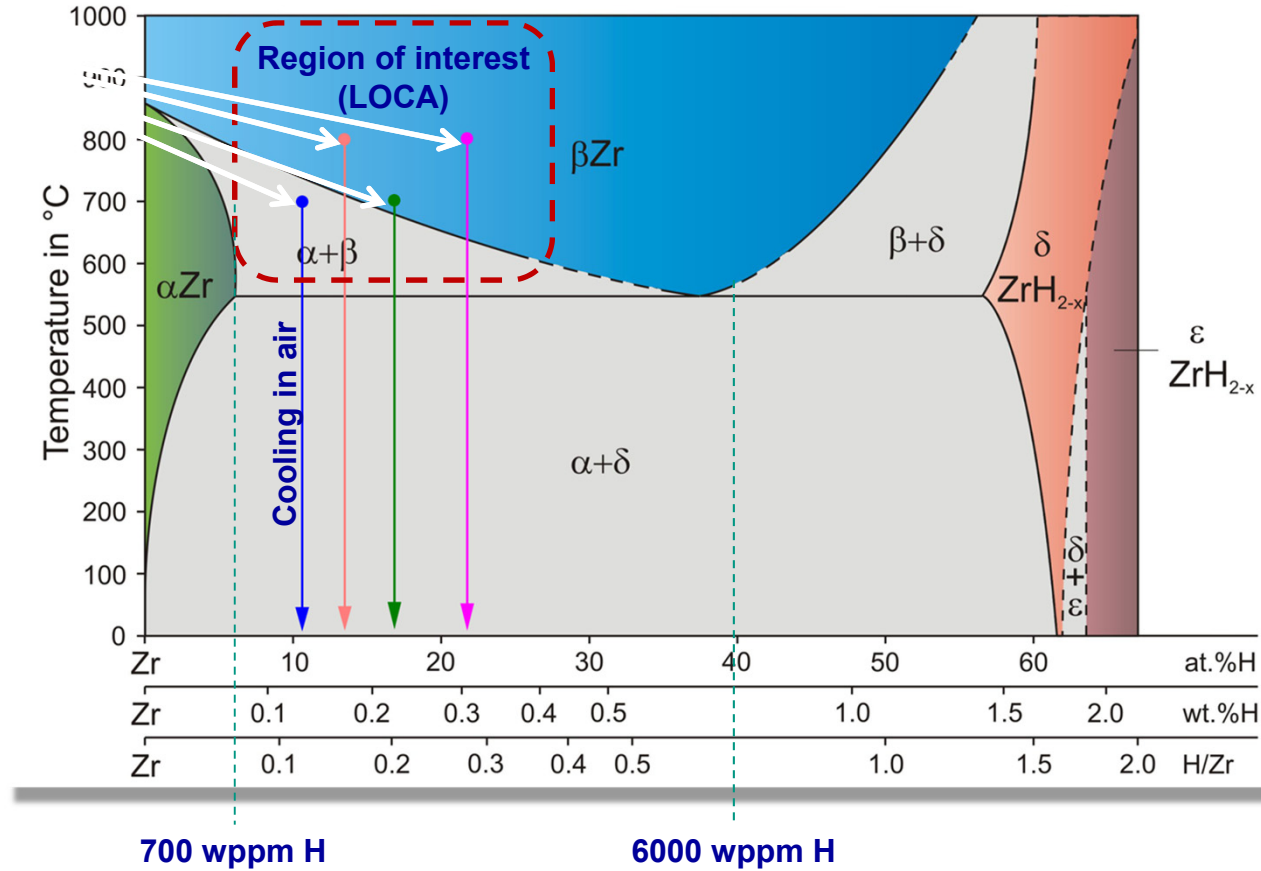
Methods of investigation:

- Hydrogenation in Ar+H₂ gas mixture in LORA tube furnace
- Metallographic investigations and microhardness tests of the tube section
- Electron back scattered diffraction analysis (EBSD) of polished and etched surfaces
- X-Ray diffraction analysis in the cladding tube wall middle
- Tensile tests with hydrogenated tube segments
- Scanning electron microscopy of fractured surfaces



Equilibrium phase diagram of Zr-H system*

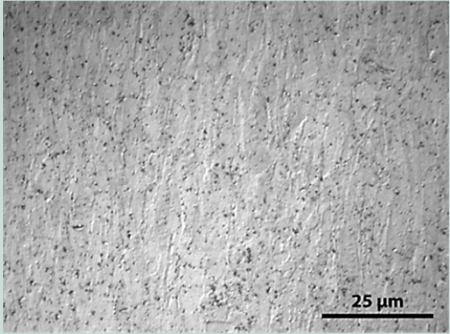
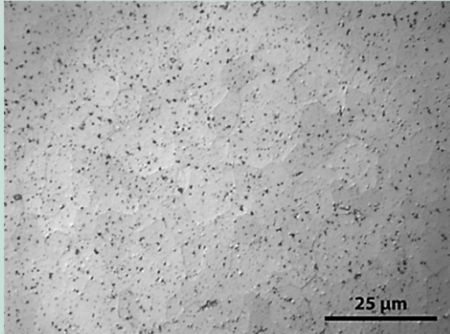
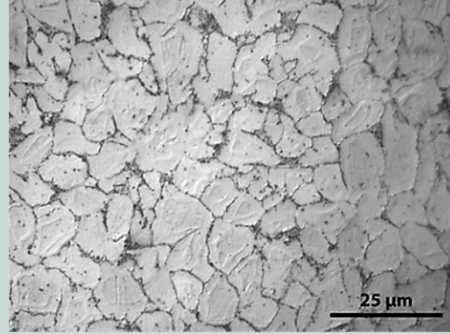
selected examples
of tests



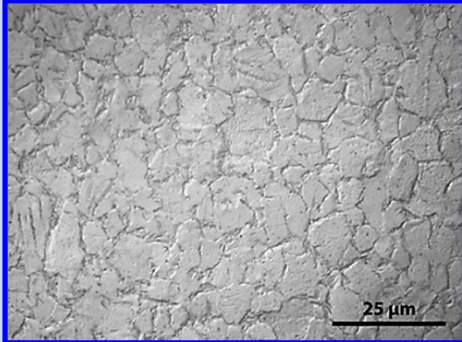
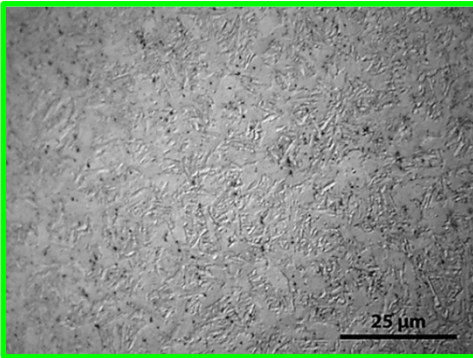
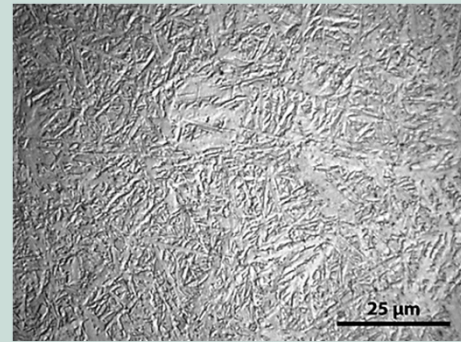
* According to E. Zuzek et al., Bull. Alloy Phase Diagr. (1990), 385

Microstructure of annealed and hydrogenated samples

Microstructure of cladding after annealing in Ar and fast cooling in air

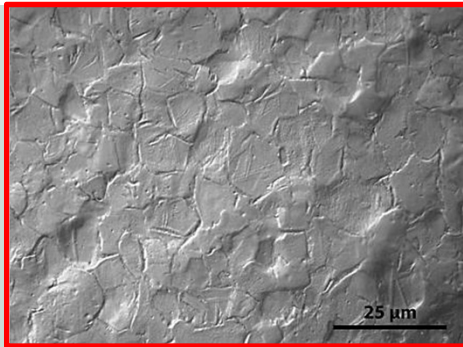
| | | |
|---|---|---|
|  |  |  |
| as-received | 600-800 °C; 480 s in Ar | 900 °C; 480 s in Ar |
| strong texturised structure | before $\alpha \rightarrow \beta$ transformation: grains tend to be equiaxed, homogeneous distribution of intermetallides (impurities) | after $\alpha \rightarrow \beta$ transformation: 1) concentration of impurities at grain boundaries; 2) needles inside grains |

Consequential development of structure (RT) for hydrogenation at 700°C

| | | |
|--|--|--|
|  |  |  |
| 1380 wppm H (120 s) | 2250 wppm H (240 s) | 4760 wppm H (720 s) |
| “non-equilibrium” grain boundaries | ≈50% of grains transformed at T into prior β -structure & formed needles at cooling | β -structure needles and few not transformed α -“islands” |

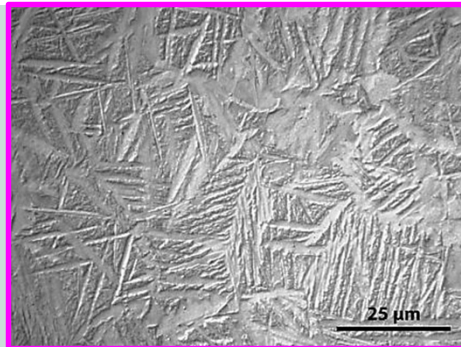
Microstructure of hydrogenated samples

Consequential development of structure (RT) for hydrogenation at 800°C



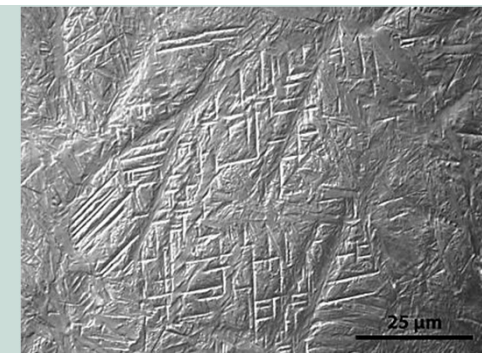
1790 wppm (120 s)

“non-equilibrium” grain boundaries



3070 wppm (240 s)

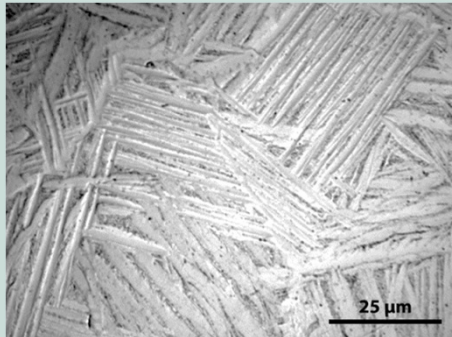
>50% of grains transformed
(prior β -structure)



8620 wppm (360 s)

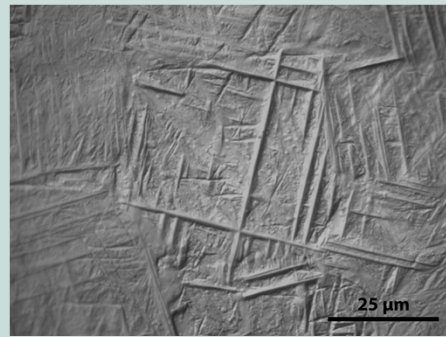
wide needles: hydrides?
narrow needles: twins?

Consequential development of structure (RT) for hydrogenation at 900°C



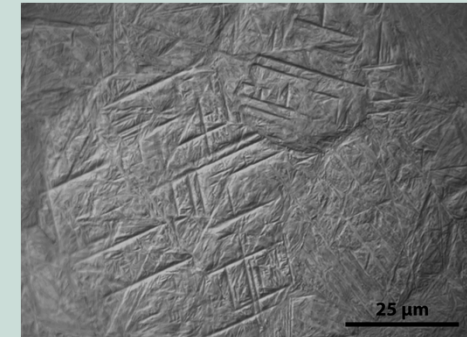
880 wppm (120 s)

all grains transformed into β -structure:
disintegration of recrystallized and
enriched with H regions into needles



2000 wppm (~150 s)

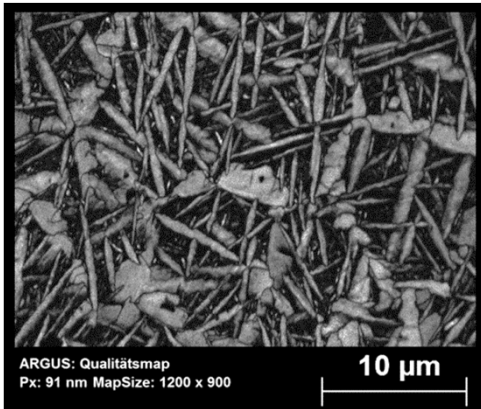
needles: hydrides or twins?



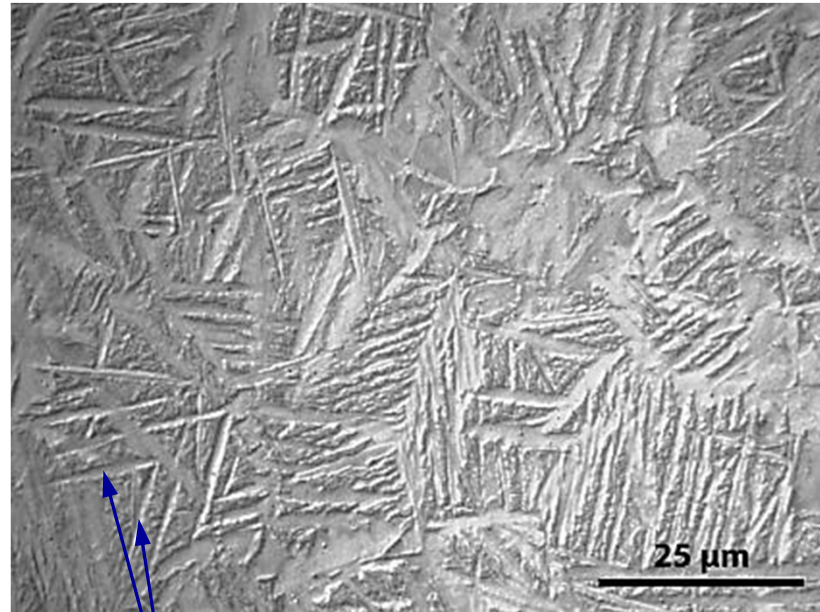
6700 wppm (240 s)

needles: hydrides or twins?

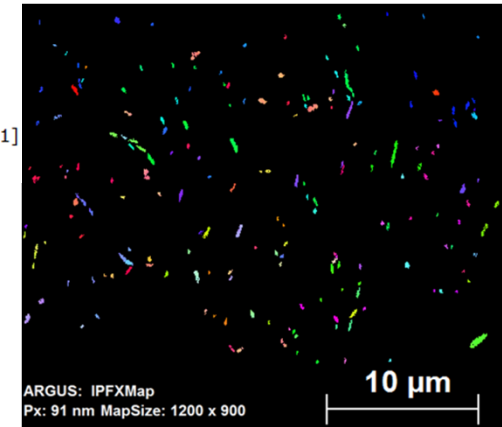
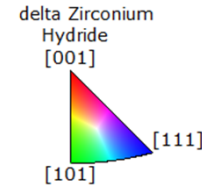
EBSD analysis of sample with 3070 wppm H (800°C)



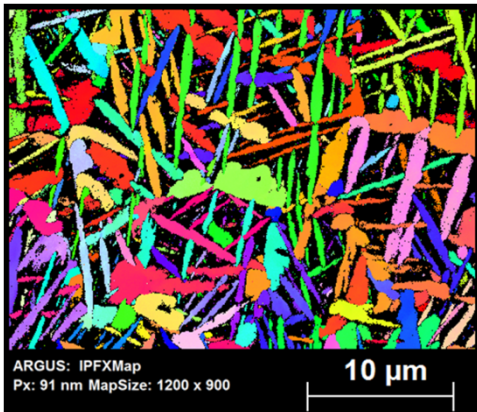
EBSD pattern quality map



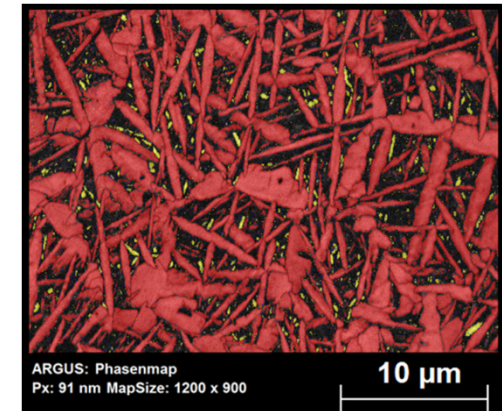
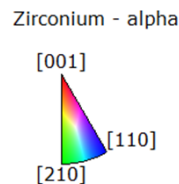
metallography:
β → α transformation occurred,
Zr-needles formation



IPF map of $ZrH_{1.6}$ regions
(cubic lattice)

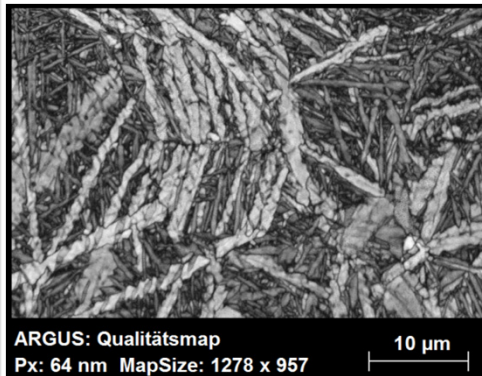


IPF map of Zr regions
(hexagonal lattice)

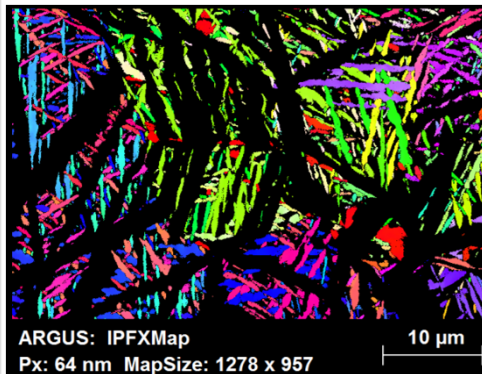


phase map:
hydride needles (yellow)
between Zr needles (red)

EBSD analysis of sample with 8600 wppm H (800°C)

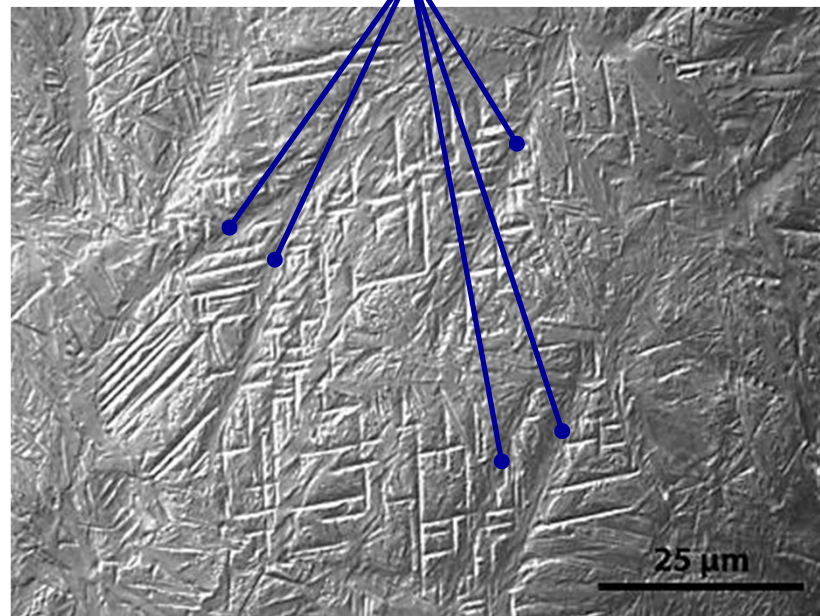
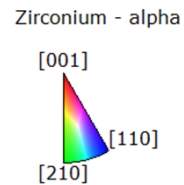


EBSD pattern quality map:
dark – Zr, light – hydrides

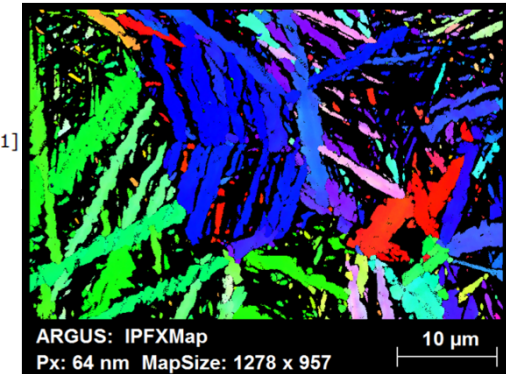
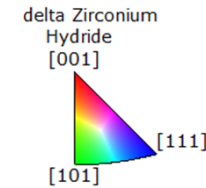


IPF map of Zr regions
(hexagonal lattice);
dark regions: hydrides

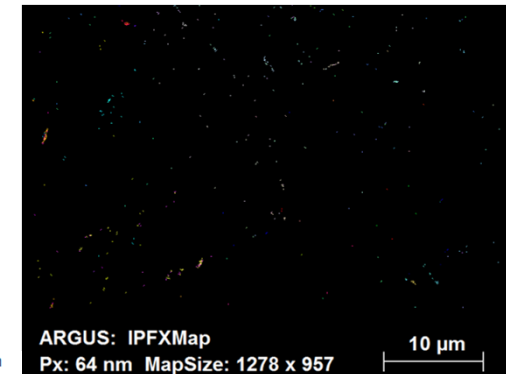
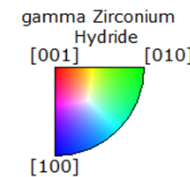
no twins were detected



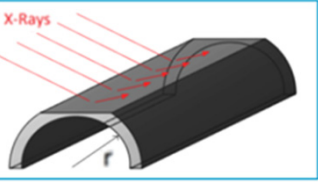
metallography:
 $\beta \rightarrow \alpha$ transformation occurred



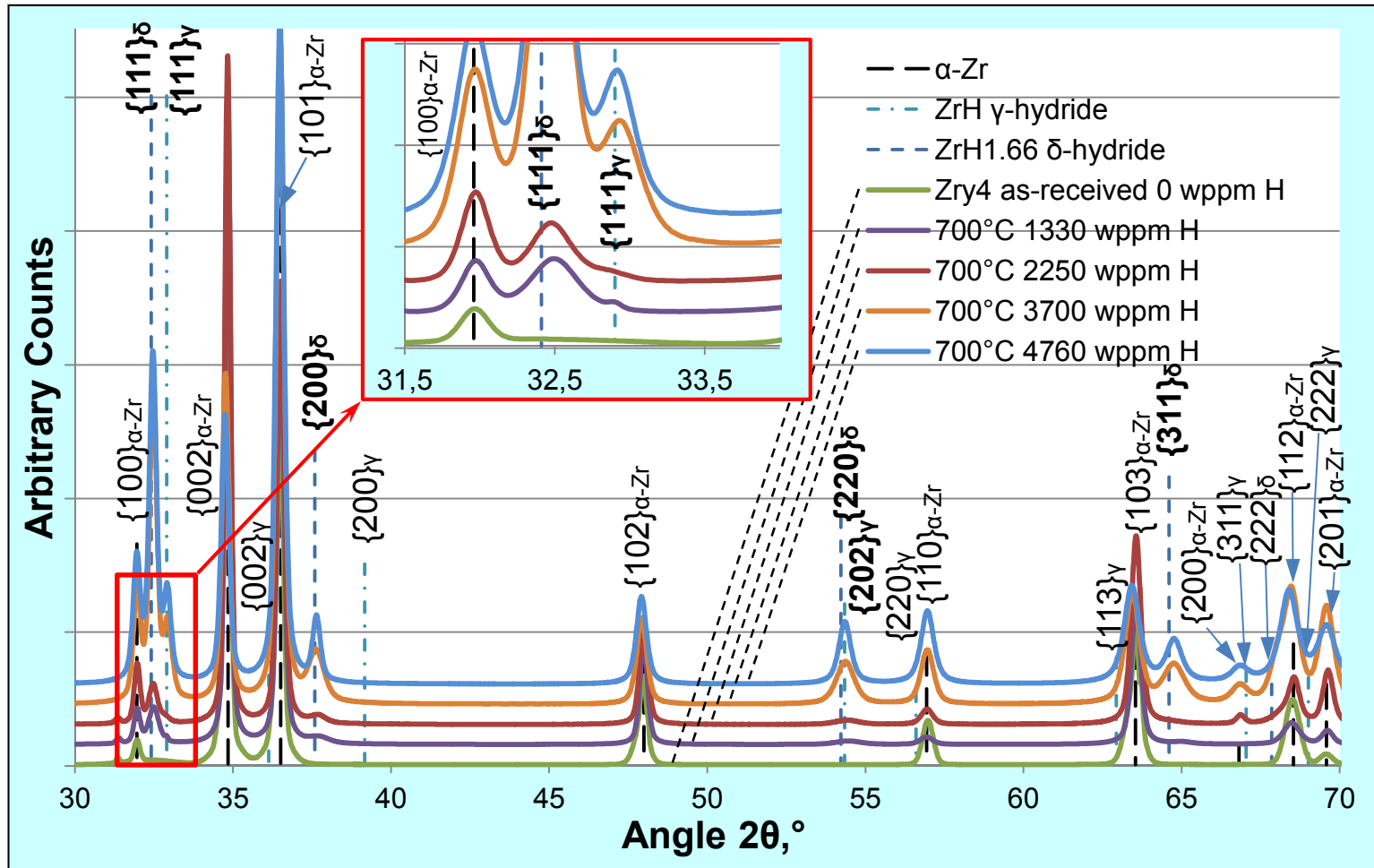
IPF map of $ZrH_{1.6}$ regions
(cubic lattice);
dark regions: Zr



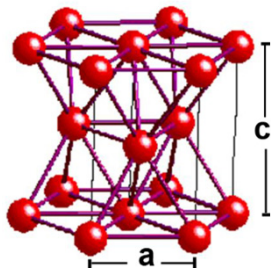
IPF map of ZrH regions
(tetragonal lattice)



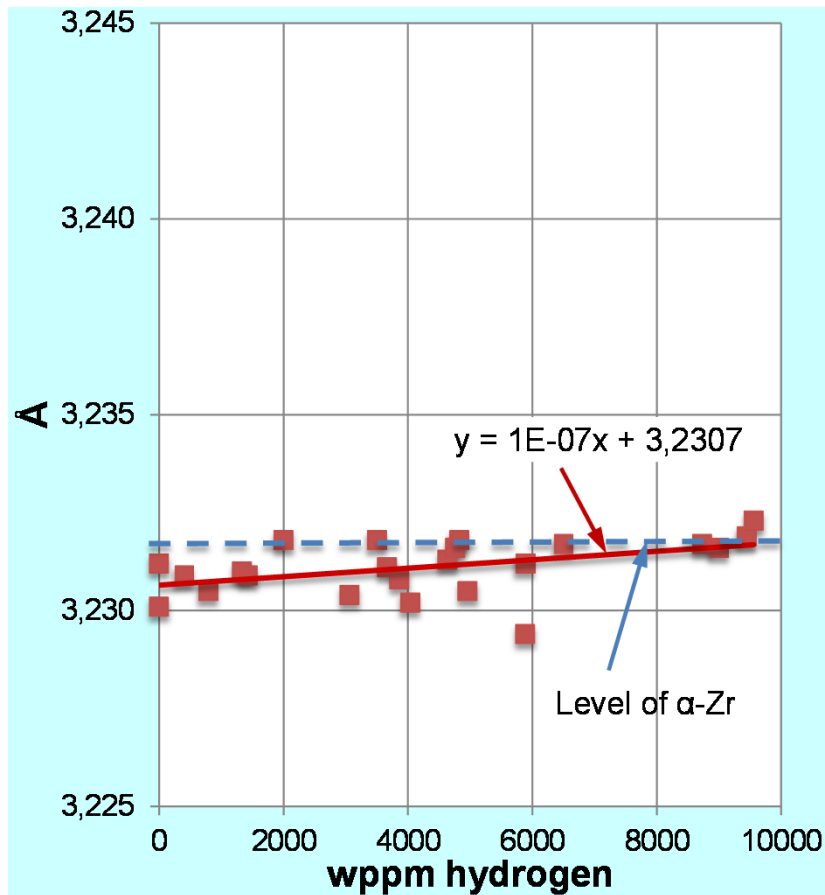
XRD analysis: detection of hydrides for Zircaloy-4 samples with more than 1000 wppm H (700°C)



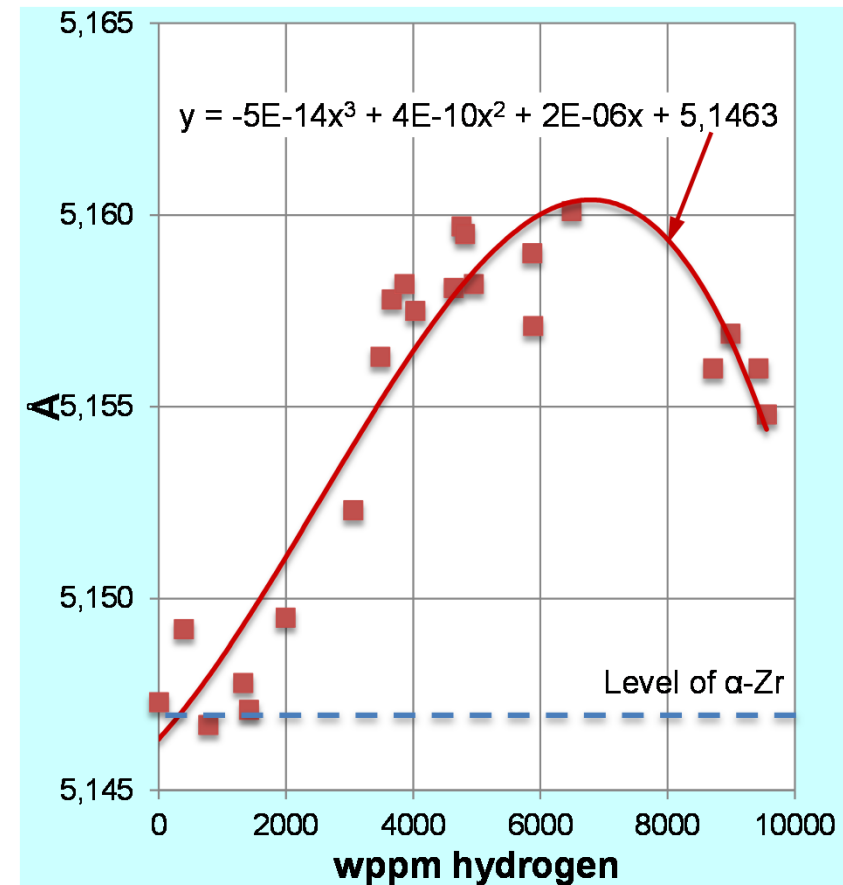
hydride peaks growth continuously with increase of hydrogen content



Calculation of Zr lattice parameters on the basis of XRD analysis: evidence of dissolved hydrogen

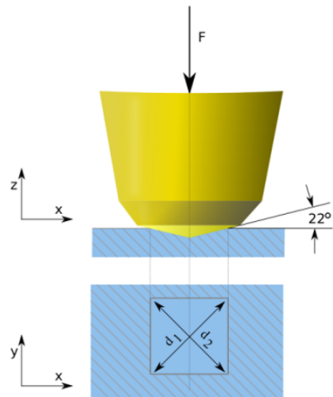


"a" corresponds to as-received material for all hydrogen contents



$C_H < 6500$ wppm: "c" increase (more dissolved H);
 $C_H > 6500$ wppm: "c" decrease (more hydride precipitation)

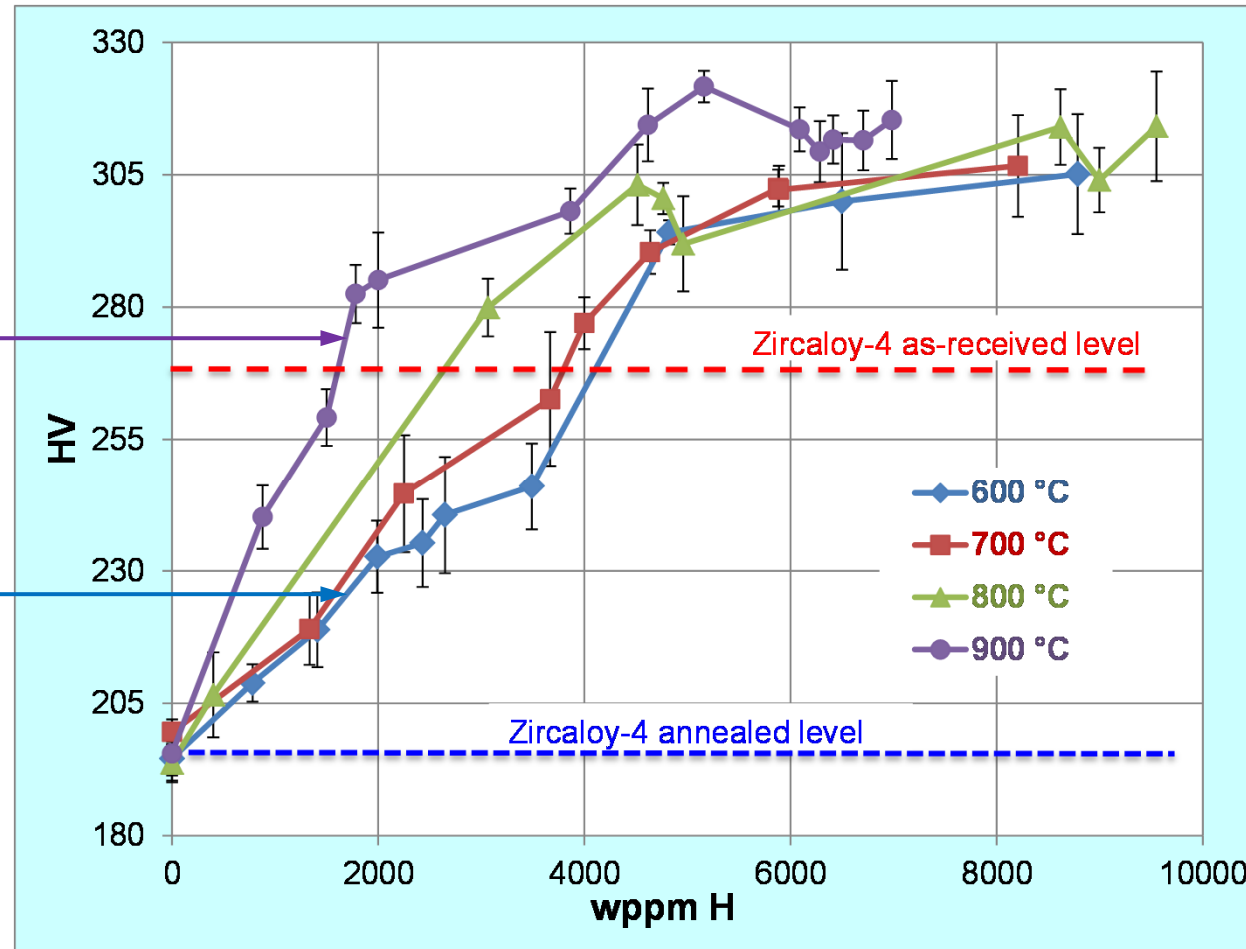
Micro hardness (Vickers) of hydrogenated Zircaloy-4 samples: dependence on the hydrogen content and temperature



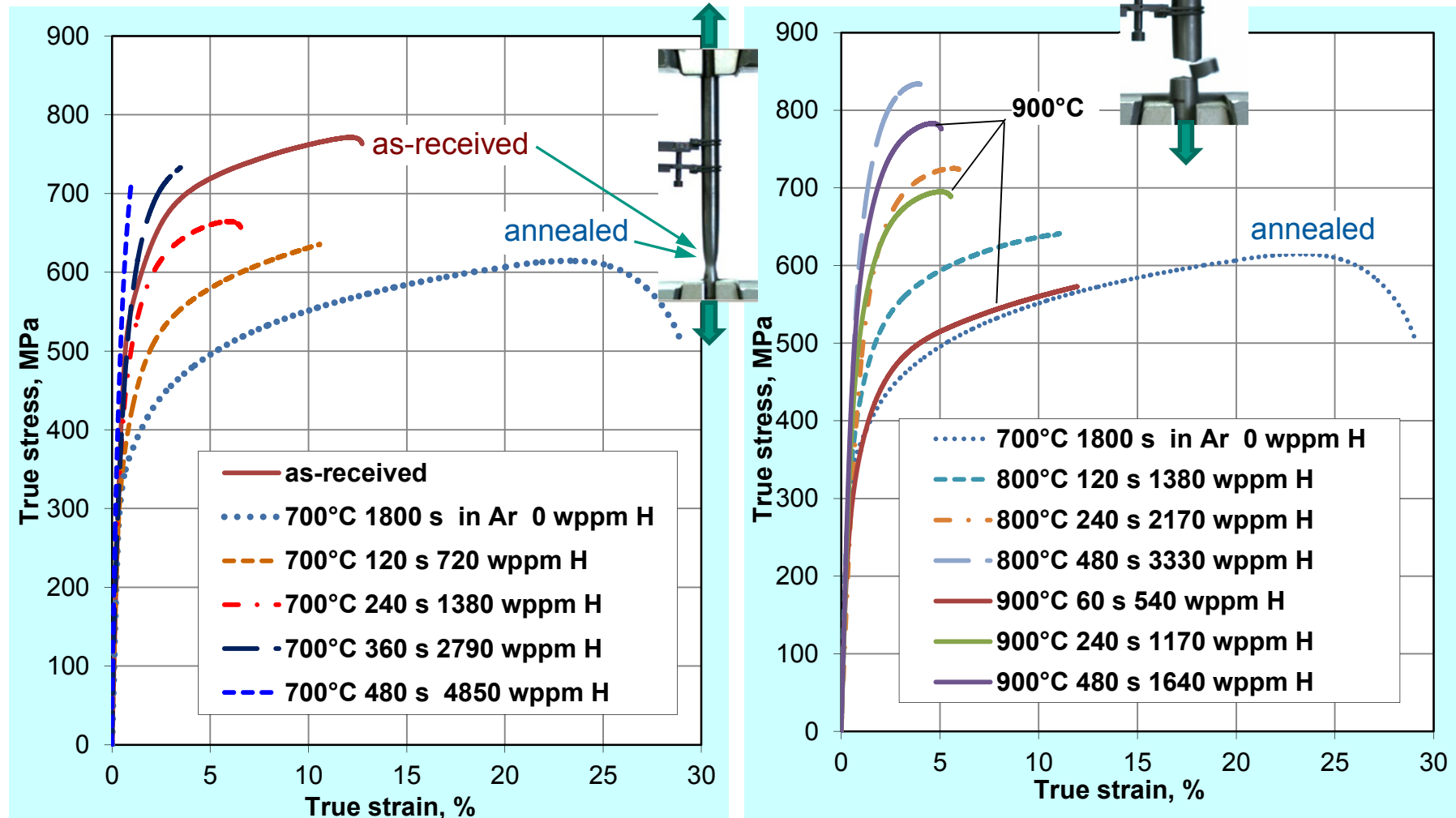
The diagonal length of resulting indented square: about 10 μm (comparable with grain sizes)

hydrogen + high temperature effect on phase transformation at 900 °C

hydrogen + low impact of temperature on phase transformation at 600 °C



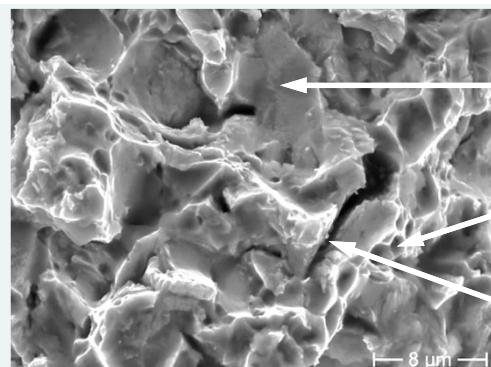
Tensile tests of tube samples (hydrogenated at 700, 800 and 900°C) at room temperature



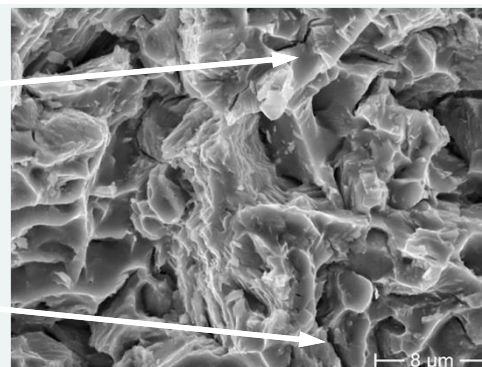
- just 700 wppm H (hydrogen mostly dissolved in matrix, only few hydrides) reduces the plasticity drastically
- the rupture was for majority of hydrogenated samples brittle

Fractured surface (SEM) after tensile tests:

- ❖ fracture is mostly brittle
- ❖ inter- and trans-granular fracture
- ❖ partially plastic deformation (micro-necking) of Zr needles

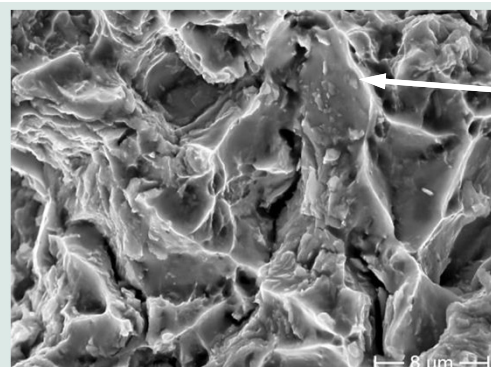


cleavage (trans-granular fracture)
few dimples
inter-granular crack

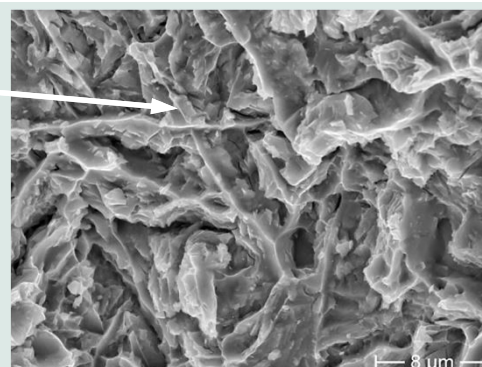


720 wppm H (hydrogenated at 700°C)

2790 wppm H (hydrogenated at 700°C)

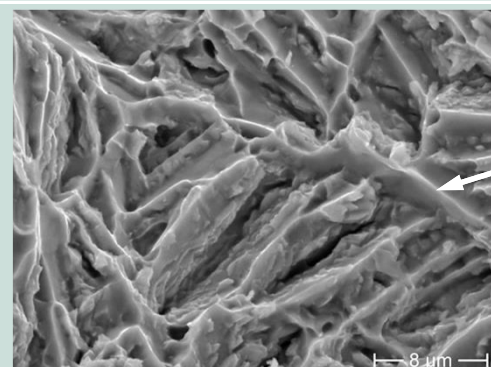


Zr needles

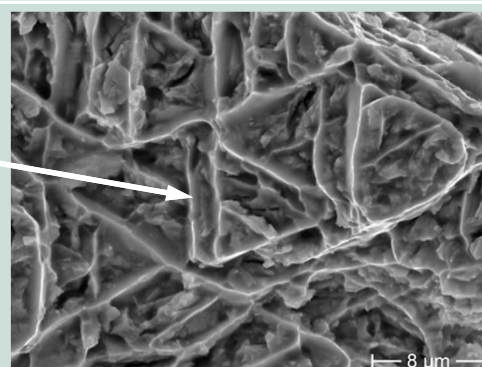


1110 wppm H (hydrogenated at 800°C)

3070 wppm H (hydrogenated at 800°C)



Zr needles



1170 wppm H (hydrogenated at 900°C)

1640 wppm H (hydrogenated at 900°C)

Summary

- No “macroscopic” hydrides were detected by means of optical microscopy after hydrogenation of Zircaloy-4 probes to 700...8000 wppm H at temperatures 700...900°C and immediate quick cooling.
- Microhardness tests showed a relationship between annealing softening and hardening (HV 190...320) due to an impact of hydrogen on $\alpha \rightarrow \beta \rightarrow$ prior β transformation and formation of hydrides during the cooling phase.
- EBSD mapping showed formation of alternated zirconium and zirconium hydride needles (with length up to 20 μm) for samples hydrogenated to above 3000 wppm H at 800°C. Distribution and orientation of γ - and δ -phases of zirconium hydrides were established.
- The XRD analysis showed the presence of γ - and δ -hydrides in all of performed experiments (700...900°C, 700...8000 wppm H). With the increase of hydrogen content the hydride peak intensities were also increased. Simultaneously the hydrogen should be partially dissolved in the lattice which is indicated by increase of the lattice parameter “c”.
- The tensile tests performed with hydrogenated cladding showed that just 700 wppm H (hydrogen mostly dissolved in matrix, only few hydrides) reduces the plasticity drastically. The rupture was for majority of hydrogenated samples brittle.

Acknowledgements

The authors would like to thank the following KIT colleagues:

- Mrs. Ursula Peters for her technical assistance with the hydrogenation tests
- Ms. Julia Lorenz for the help during preparation of the specimens for metallographic observations
- Dr. Harald Leiste for carrying out of X-Ray diffraction measurements
- Dr. Marcus Müller for carrying out of FEG-SEM observations

Thank you for your attention!

<http://www.iam.kit.edu/wpt/471.php>

<http://www.iam.kit.edu/wbm/552.php>